Environmental Science
Water Research & Technology

ROYAL SOCIETY OF CHEMISTRY

PAPER

View Article Online
View Journal | View Issue

Cite this: *Environ. Sci.: Water Res. Technol.*, 2021, **7**, 2372

Filter-less separation technique for micronized anthropogenic polymers from artificial seawater

Lucas Grob, *[a] Liridon Zeneli,[a] Eileen Ott,[a] Jacopo Vialetto,[b] Jotam Bergfreund,[a] Yasushi Takeda[a] and Erich J. Windhab*[a]

Anthropogenic polymer particulates (APPs) are a highly researched topic, from the identification of their different sources to their impact on living organisms, and micronized anthropogenic polymers pose a threat to many ecosystems. Prevalently found are microplastics (MPs) including PMMA. Additionally, micronized rubber powder (MRP), which originates from tire abrasion but is also used as a filler material for various other products, can be found. Due to their small size of less than 100 μm in diameter and relatively low concentrations found in wastewater or seawater, the cleaning from such water sources of MPs or MRP will only be of technological and economic relevance if an efficient, low cost pre-concentration step can be applied before other filtration/separation technologies are applied. Flotation is expected to be such a relevant pre-concentration technique if a high enough affinity of MP/MRP particles to gas bubbles would exist. Accordingly the interaction behavior of MRP and MPs with such gas bubble interfaces was investigated. Based on this, a simple, fast and filter-less technique was developed to remove APPs from seawater by a newly designed process combining flotation and separation in a hydrocyclone type setup. In a first step, we characterized the MRP and found two particle fractions with different gas bubble interaction behaviors. One fraction formed spontaneous air bubble–particle clusters and was prone to attach to the air–water interface. The second fraction sedimented and accumulated at the bottom. Once adsorbed at the interface, the particles remained irreversibly attached. Both MPs and MRP stabilized the foams from air bubbles in artificial seawater as well as in MilliQ water, indicating a preferred localization at the air–water interface. Thus, when treated in the modified hydrocyclone (mHC) based flotation process with controlled swirl flow applied, an extraction ratio of 26% was reached, whereas without bubbles, only 3.7% was reached. The investigated model mHC enabled us to concentrate and separate APPs, in the diameter range $d_{90,3} \leq 105$ μm with particle density very close to water, with the use of their promotion of the air–water interface. These promising results in a first test step for our system encourage further investigation of the applied technology for microplastic-contaminated water.

Received 4th August 2021,
Accepted 4th October 2021

DOI: 10.1039/d1ew00553g

rsc.li/es-water

Water impact

This newly designed separation processing principle demonstrates how microplastics with hydrophobic tendencies and low density differences to the medium can be separated or up-concentrated in an efficient way without the use of filters. This technique shows high potential to serve as a pre-treatment step before subsequent filtration of wastewater containing microplastics.

Introduction

Anthropogenic polymer particulates (APPs) can be divided into two different categories: thermoplastics and thermosets.[1] Due to abrasion and inadequate waste management, micronized APPs are ubiquitous. Micronized thermoplastics are commonly known as microplastics (MPs) including synthetic precursors like polyethylene, polystyrene, and poly(methyl methacrylate) (PMMA), and others, which are typically smaller than 5 mm in size,[2,3] with different colors and shapes. It has been reported that 80% of MPs in our freshwater and seawater are from terrestrial sources.[4] The typical concentration in seawater ranges from *ca.* 10 to 500 particles per m^3 depending on the location. Most abundant MPs are from polyethylene and polystyrene.[5] Their ubiquitous abundance has also been shown to have a pronounced negative effect on smaller life forms, as

[a] *Laboratory of Food Process Engineering, Department of Health Science and Technology, ETH Zürich, Zürich, Switzerland. E-mail: lucas.grob@gmx.ch*
[b] *Laboratory for Soft Materials and Interfaces, Department of Materials, ETH Zürich, Zürich, Switzerland*

inclusions of MPs in algae cells were found.[6,7] Within the collected APP samples from seawater, the occurrence of micronized rubber powder (MRP), often referred to as tyre wear particles, has also been reported.[8] MRP is an umbrella name for the abrasion of thermoset polymers. Similar to MPs, MRP is found in every land compartment[9] and river water at concentrations of 0.5–5 mg L^{-1}.[8]

The driving force for the sedimentation or flotation behavior of APPs in a static water body is the density difference. The density of APPs typically ranges from 0.85–1.45 g cm^{-3} for MPs[10] and 1.15–1.20 g cm^{-3} for MRP.[11] Accordingly, this results in a rising/sinking velocity of a particle (d_p = 105 μm) in still water at 25 °C of approximately 0.012 and −0.025 m s^{-1} for densities of 0.85 and 1.45 g cm^{-3}, respectively, according to calculations based on the dimensionless Archimedes (Ar)–Omega (Ω) relationship. The most common techniques to separate particles by size and substances, apart from using filters, include hydrocyclones and froth flotation applications. In a hydrocyclone, the observed particle separation is a result of an opposing centrifugal and drag force balance.[12] The suspension is tangentially led into an upper cylindrical inlet section thus generating a helical swirl flow of a certain angular velocity and entering into the conical cyclone section at its lower part. This results in the movement of larger particles towards the cyclone wall. Froth flotation is used to *e.g.* extract valuable mineral particles from a liquid medium. Air is purged into a pulp of particles in water, which is conditioned with a small amount of surface active reagents. This leads to formation of bubbles which then collide with particles, thus getting attached to the floating bubble interfaces and forming a stable froth on top of the liquid surface. Often, a so-called collector is added to render one mineral selectively hydrophobic and thus increase the collection efficiency.

The extraction consistency and lack of filter-less techniques to filter large volumes of water to obtain APPs are a well-known problem.[13] Only a few researchers have published other separation methods, such as elutriation,[14] to concentrate watery suspensions of APPs. In the presented work, we explored a separation technology combining flotation and centrifugal separation within a modified hydrocyclone device.

Experimental

Materials

Anthropogenic particles. Micronized rubber powder (MRP) was obtained from Entech, Middlebury, IN, USA. The MRP was then further sieved (Fritsch Analysette 3, Fritsch GmbH, Idar-Oberstein, Germany) to access smaller size fractions. As an MP, poly(methyl methacrylate) (PMMA) esplas H60 from KSL, Staubtechnik GmbH, Germany, was used.

Modified hydrocyclone design. A modified hydrocyclone (mHC) was designed according to the schematic drawing shown in Fig. 1 with the dimensions given in Table 1. The throughput $\dot{Q}$ was set to 33.7 L h^{-1}. In addition, an air inlet

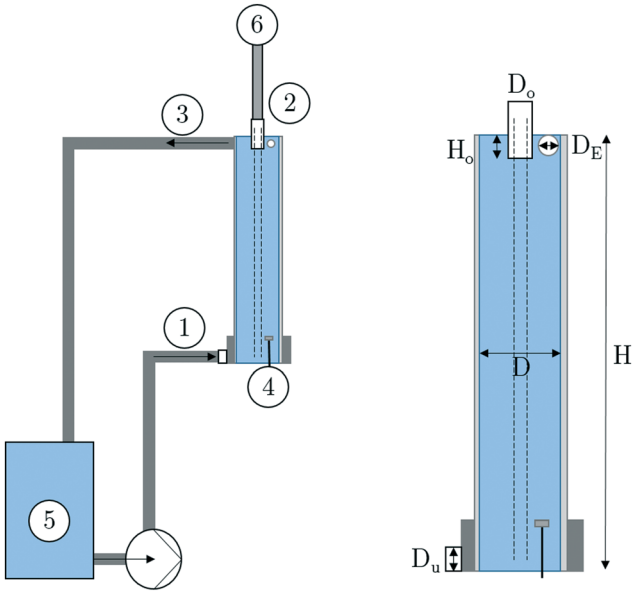

Fig. 1 Modified hydrocyclone design. 1. Inlet, 2. outlet of separated particle loaded foam, 3. outlet cycle, 4. air inlet, 5. storage container, 6. sampling station.

with a sintered metal membrane (max. pore size p = 3 μm, d_m = 20 mm) was built into the hydrocyclone at a height of 10 cm from the bottom and a distance of 5 cm from the center of the cylinder. The air flow was fixed at 50 mL min^{-1} and controlled using a flow meter (GCR-B4SA-BA15 red-y, Vögtlin Instruments AG).

Methods

Particle characterization. The particle sizes were assessed with laser diffraction analysis (Beckman Coulter LS 13320, Brea, USA). 10 wt% particles were suspended in medium chain triglyceride oil (MCT, WITARIX MCT 60/40, IOI Oleo GmbH, Hamburg, Germany) and ultrasonicated at 200 W at 24 kHz with a maximum amplitude of 175 μm for 2.5 min (Hielscher Ultrasonics GmbH, Teltow, Germany). The particle density was measured with a pycnometer (AccuPyc II 1340, Micromeritics, Norcross, Georgia, USA). As purge gas helium was used with a fill pressure of 19.5 psig, 25 cycles were conducted with an end equilibration of 0.005 psig min^{-1}.

Particle behavior in medium. To characterize the behavior in MilliQ water, 100 mg of MRP or PMMA was mixed in 50 ml MilliQ water. The suspension was then vortexed for 90 s. After five minutes the top fraction was extracted with a

Table 1 Dimensions of the hydrocyclone

D	0.15 m
H	0.895 m
D_E	0.04 m
D_o	0.05 m
H_o	0.06 m
D_u	0.05 m

spatula, dried and weighed before filtering the bottom fraction with a coffee filter. For PMMA, no quantification was possible. Measurements were performed in triplicate (N = 3).

Gel trapping technique. The gel trapping technique allows us to image and analyse the wettability of colloidal particles adsorbed at fluid interfaces. The experimental procedure is as follows.[15] In a glass beaker, 2 wt% of gellan gum (GELZAN™ CM, Sigma-Aldrich) was dissolved in MilliQ water at 70 °C. MRP particles were dispersed in MilliQ water and injected with a glass syringe at the hot air/water interface. After 5 min of equilibration, the sample was slowly cooled down to set the gel and immobilize the adsorbed particles at the interface. After 24 h, the gelled water surface was imaged with an optical profilometer.

Optical profilometer. MRP particles immobilized at the gelled water surface were imaged with an optical profilometer (Plu Neox, Sensofar, Terrassa Spain) in bright field mode. A 20× objective (LU Plan Fluor, Nikon) was used for imaging. The topography image of the interface allowed for imaging only the surface of the particle protruding out of the gelled water surface. At the same time, a reflection microscopy image was recorded in order to visualize also the surface of the particle immersed in the gel. Topography images were then analyzed with the software Gwyddion.

Static foaming. To examine the effect of MRP or MPs on foam stability, a glass column (d = 4.5 cm) with a sintered glass filter (p = 40 μm) at the bottom was set in a beaker filled with the medium. The air flow was kept constant at 1.5 L min^{-1} for three seconds. To ensure isothermal conditions, the beaker was tempered at 25 °C. Three different watery media were tested: MilliQ water, tap water, and artificial seawater (ASW),[16] and to mimic the surface active microlayer on the sea surface, 0.2 mg L^{-1} surfactant (Triton X-100, Sigma Aldrich, Switzerland) was added. Each medium was tested with and without the addition of MRP or MPs ($d_{90,3}$) and this was repeated three times. The foam height experiments were recorded and analyzed using the ImageJ software with the Fiji manual tracking plugin. Each individual experiment produced a curve of the foam height over a time period of three seconds. A plateau of the foam height was visible, as shown in Fig. 2B. For the calculations, the plateau height was used. The relative mean height was calculated as the ratio between the measured foam height with the addition of particles and the measured foam height without the addition of particles in the aforementioned medium ($H_{0,\mathrm{medium}}$).

Ultrasonic velocity profiling (UVP) of the hydrocyclone. Ultrasonic velocity profile measurements were carried out with an ultrasound Doppler, immersion type transducer at 4 MHz with 5 mm active element (TN and TX-line, Imasonic, Besançon, France) and a UVP-DUO profiler (Met-flow SA, Lausanne, Switzerland).The sensors were positioned every 5 cm over the cylinder height starting at 125 mm from the bottom crossing the centerline or 1 cm offset to the centerline of the hydrocyclone (see Fig. 3). Measurements were performed with a maximal distance of 160 mm and a resolution of 0.56 mm per voxel. Further details can be obtained here.[17]

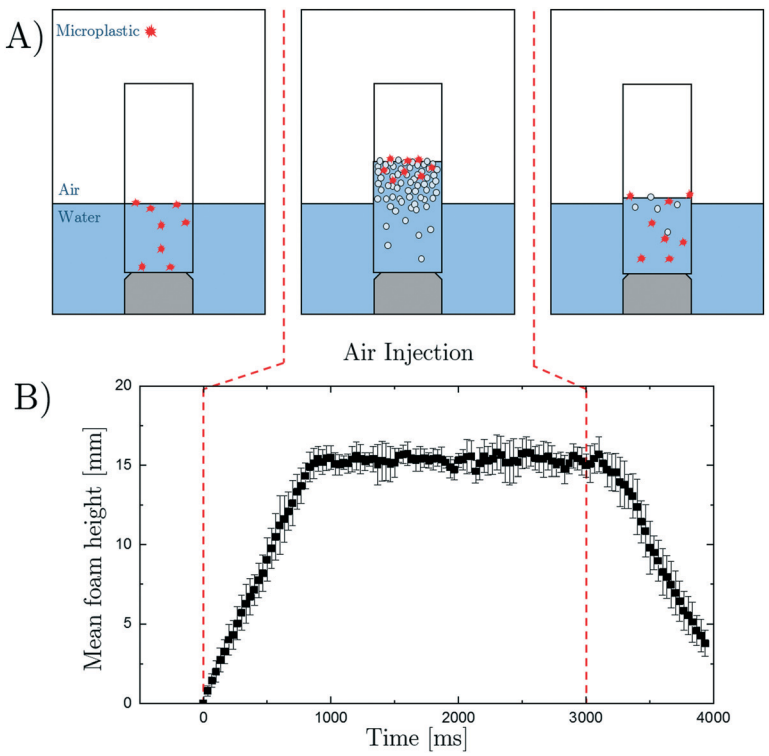

Fig. 2 Foaming experiment setup: A) microplastic particles were added to the glass column. Then air was injected and the foam height rose. Air injection was then stopped and the foam height decreased again. B) The increase in foam height with a subsequent plateau in foam height.

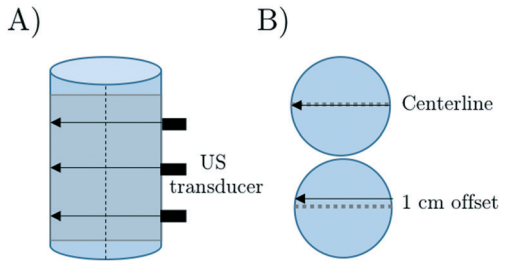

Fig. 3 Ultrasonic velocity profiling (UVP) measurement setup. A: Side view of the modified hydrocyclone and attached US transducers. B: Top view centerline and 1 cm offset measurement.

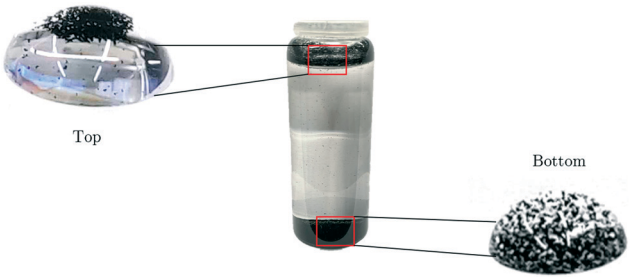

Fig. 4 Visualisation of particle separation from an MRP suspension, $d_{90,3}$, at a concentration of 2 g l^{-1} in MilliQ water, vortexed for 90 s with a waiting period of 5 min.

Particle addition and extraction to the hydrocyclone. To test the hydrocyclone separation capacity, the washed APPs were added with a syringe to ASW (V = 100 L). A concentration of 3.35 mg L^{-1} of MRP or MPs was tested. 20 mL of medium was extracted at heights of 725, 675 and 625 mm (denoted as A, B and C). The number of particles was counted ($N_{counted}$) and the efficiency ratio was calculated according to eqn (1):

$$\frac{N_{counted}}{N_{total}} = \frac{N_{counted}}{\frac{c}{\rho \cdot 4/3\pi \cdot r^3}} \quad (1)$$

To assess the extraction over time, the particles were extracted at 725 mm after 0, 5, 15, 30 and 60 min. After each time step, the particles were reintroduced into the process. All measurements were performed in triplicate.

Statistical analysis. A Kruskal–Wallis ANOVA test computed with IBM SPSS Statistics 24 was performed. The significance level was set at 0.05.

Results and discussion

I. Cluster formation of MRP

As reported by various researchers, leaching of surface active substances such as zinc and polycyclic aromatic hydrocarbons is common when APPs, especially MRP, are re-introduced into water.[11,18,19] Such leaching of interfacially active components and the related reduction of surface tension of the supernatant were also found due to a washing effect applied to the MRP particles. In a follow-up step, the washed and classified MRP fractions were re-introduced into MilliQ water (see Fig. 4). After processing and settling for 5 minutes, two major fractions were collected at the top and bottom of the cylindrical vessel used and were weighed. In Table 2, the ratios between the two fractions of MRP samples with different mean particle sizes $d_{90,3}$ (n = 4) are shown. Larger fractions of up to 5.2 times more particles were found at the top of the vessel than at the bottom. The top particle fraction was removed and the subsequent mixing step applied to the bottom fraction did not lead to another separation at the top.

To visualize the observed behavior, Fig. 5 shows the microscopy images of particles extracted from the top and bottom separated fractions from different water sources

Table 2 MRP bottom and top separation ratios in MilliQ water (n = 4)

MRP mean particle size $d_{90,3}$ [μm]	Top (a) [mg]	Bottom (b) [mg]	Ratio a/b [w/w]
105	51.63 ± 13.26	11.47 ± 3.85	5.2 ± 2.6
<32	43.33 ± 5.3	17.44 ± 5.92	2.9 ± 1.9
25 < × < 32	42.05 ± 2.52	19.84 ± 9.64	2.4 ± 0.9

being MilliQ water, tap water and artificial seawater (ASW). The particles from the top fraction were aggregated at the air–water bubble interface. Pycnometric measurements of this particle fraction showed a density of about 1 g cm^{-3}. In addition, the method suggested closed porous structures of approximately 72.3% v/v. Similar behavior, as found on top, was reported as an alternative way to fight oil spills.[20] In such a case, the aggregated particle clusters exhibit large capillary forces used to immobilize oil. In contrast to PMMA, such a type of cluster formation was not observed and no top layer separation could be carried out. Further it was noted that the particle size of APPs did not significantly increase when introduced to the watery medium. Thus swelling of the porous structure could be neglected.

When particles were immobilized by gelling the water phase, both fractions of particles from the bottom and top were shown to protrude in the entrapped gas phase, as shown in Fig. 6A) as dark and in Fig. 6B) as bright areas. The contact angle or protruding area in the air phase remains low for spontaneous from-bulk adsorption because of pinning of the contact line on the rough and porous surface. Therefore the measured protruding area is not correlated to the thermodynamic contact angle value in equilibrium.[21,22] The energy required to desorb a particle from the fluid interface can be expressed as:

$$E = S \cdot \gamma \quad (2)$$

where S is the cross-section surface area of the protruding part of the particle in the air phase, and γ denotes the interfacial tension (72 mN m^{-1} for air/water). From the gel trapping experiments, we obtained an average height of protruding particles into the gas of $h_{max} \approx 1$ μm and a related average interfacial area of the particle protruding in

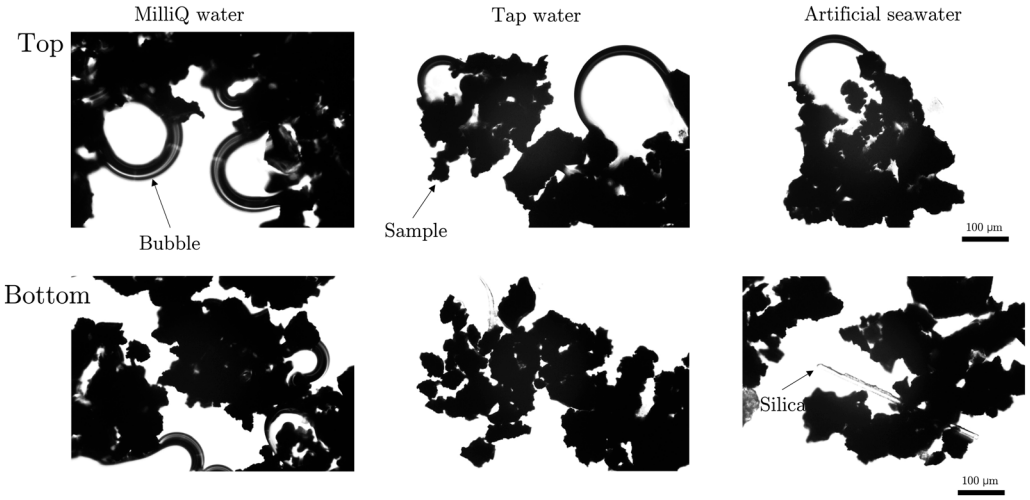

Fig. 5 Light microscopy images of MRP at 2 g l^{-1}, in different watery media (MilliQ water, tap water and ASW). Samples from the top and bottom extracted after 5 min of vortex and 5 min of settling.

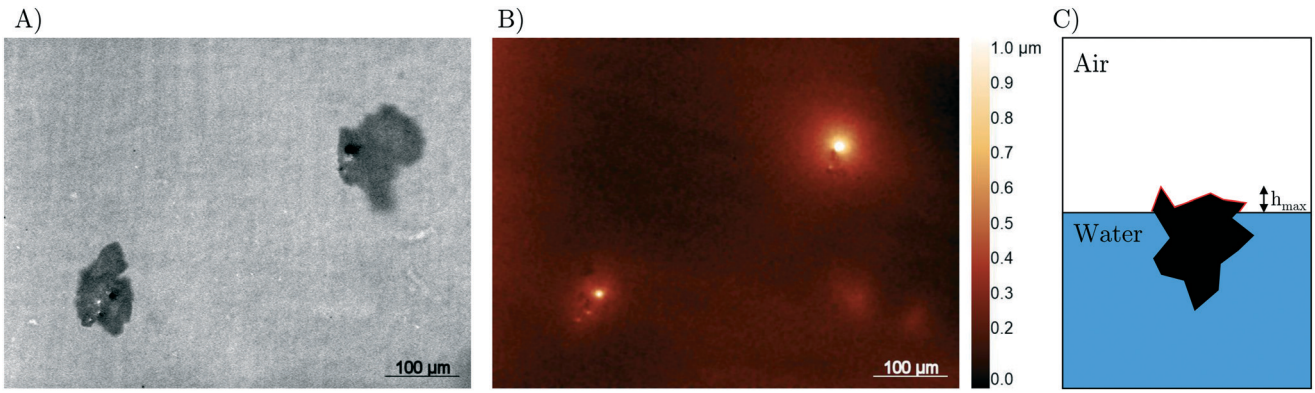

Fig. 6 Particles extracted from the top separated fraction immobilized at the air–water interface in the gelled water phase. A) Reflection light microscopy image. B) Corresponding optical profilometry image of the gelled water surface. C) Schematic drawing of a particle protruding at a maximum height h_{max} in the air phase with an outlined surface area (red).

the air phase of S = 1000–5000 µm^2. In conclusion, for an average surface area of S = 3000 µm^2 the energy required to desorb a protruding particle is calculated to be $E \approx 5 \times 10^{10}$ k_BT. Thus, the particle will remain irreversibly attached once adsorbed at the fluid–gas interface. Consequently, forcing particle adsorption through foaming should enable collection of all particles adsorbed at the fluid–gas interface.

In summary, if particle–interface contacts are promoted, once adsorbed at the interface due to their wetting properties, and supported by their rough and porous surface, particles remain irreversibly attached. For the separated top particle fraction, gas bubble/particle interaction happens spontaneously, while it requires mixing energy for sedimented particles from the bottom.

II. Foam stability

The findings from Fig. 6 suggest that the particles stabilize the air–water interface. Following this indication, static foaming with and without particles in different media was performed in a foam formation column. The obtained steady state foam height was divided by the height without addition of particles. Fig. 7 shows this relative foam height ($H/H_{0,medium}$) as a function of the mean particle size $d_{90,3}$. A relative foam height ratio larger than 1 indicates a constructive influence of the particles on foam stability, whereas a ratio smaller than 1 indicates foam deconstruction by the particles. Surprisingly, the $H/H_{0,medium}$ increased when particles were added to MilliQ water and ASW. This effect is explained by the hydrophobic nature of the APPs. Moreover, the water drainage in the lamellas was delayed by the addition of particles. In contrast, the $H/H_{0,medium}$ of tap water was reduced below 1 due to gradual collapse of the foam. Water molecules close to a hydrophilic surface have a strong attractive interaction with surface atoms, *e.g. via* hydrogen bonds, increasing the surface free energy. This interaction also leads to structuring of the "interfacial water" and consequently water molecules on average reside longer at

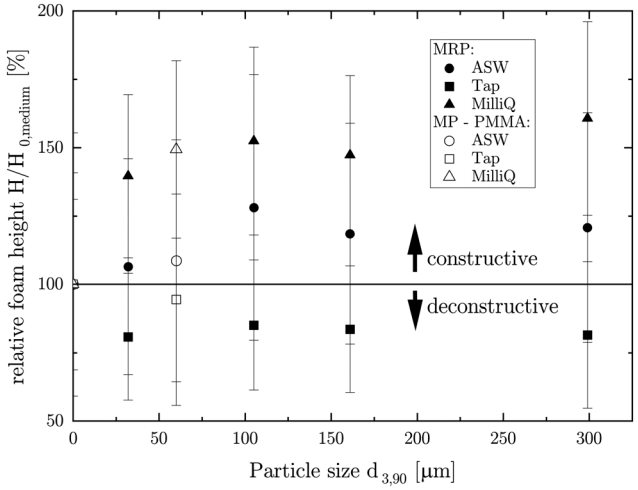

Fig. 7 Relative foam height $H/H_{0,\mathrm{medium}}$ as a function of added APPs of a specific size $d_{90,3}$. The particles were MRP and MP-PMMA added to MilliQ water, tap water and artificial seawater (ASW).

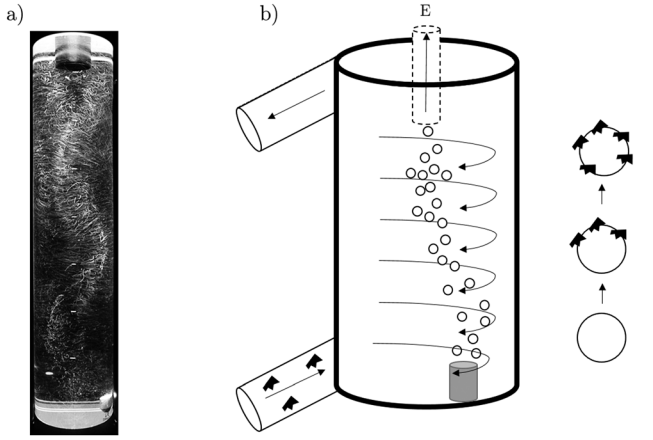

Fig. 8 Exemplary picture of the overall flow pattern (a) and its schematic representation (b) within the modified hydrocyclone. Watery medium including APP streams tangentially introduced at the bottom. Additional air flow through a membrane (gray) to create a helical bubbly co-flow. Up-concentration and extraction of the particles at point E.

positions with strong interaction than at positions with lower interaction force.[23] Dissolved ions may alter the water structure, particle surface wettability and colloidal interaction between bubbles and particles.[24] Large inorganic ions such as Ca^{+} and I^{-} are considered as "structure breaking" ions. These ions are predominant in the tap water, leading to the observed destructive phenomenon. Meanwhile "structure making" small inorganic ions such as Mg^{2+} and Cl^{-} can be found in the ASW. Moreover it was shown that destabilisation of hydration layers surrounding coal particles increased their surface hydrophobicity.[25] Thus it was suggested that the use of inorganic salts could compress the double layer around the particles resulting in opening of hydrophobic sites. These sites may then attract equally more hydrophobic bubbles compared to the watery bulk phase and stabilize at their interfaces.

III. Separation efficiency of APPs in artificial seawater

The presented filter-less technique relates to a modified hydrocyclone (mHC). To separate the suspended particles of low density difference to the watery fluid phase from artificial seawater, the mHC was operated at 33.7 L min^{-1}. In contrast to the common hydrocyclone design, this design purely consisted of a cylindrical body instead of a cylindrical top connected to a conical bottom. The fluid inlet was tangential to the cylindrical body to generate a helical upward swirl flow. In addition, a bubbly co-flow was introduced through a membrane. Taking into account the previously explored effects of foam stabilization, an increased air–water interface in combination with the helical complex swirl flow was expected to increase the "particle capturing capabilities", thus supporting the generation of a stabilized particle. The schematic flow and the complex particle capturing mechanism introduced by floating bubbles are presented in Fig. 8. The separation efficiency refers to the process of capturing particles by individual bubbles and as a result of superimposed collision, attachment and detachment events.[26] Moreover, in a typical flotation process, particle–bubble collision and additional adsorption of surface active agents may happen simultaneously. A zone model, with the accumulation of surface active agents at the rear end of the bubbles, was also proposed.[27] Thus, the size of the bubbles in relation to the size of the particles,[28] rising bubble relative velocity, surface active agents present and the local hydrodynamics[29] determine the particle collection efficiency.

To characterize the flow field within the mHC, ultrasound Doppler velocimetry flow mapping with bubbles acting as tracers was applied, a spatio-temporal velocity map measured in a non-invasive way.[30] The average radial velocities along the ultrasonic beamline over the height of the mHC are mapped in Fig. 9. When a measurement line of 1 cm offset from the centerline was applied, the swirl character became apparent. Therefore, alternating velocities pointing away and towards the beam direction were typically detected, characterizing the S-shape characteristics of the hydrocyclone shown in Fig. 8a and b. Further detailed characterization of the swirl flow motion and fluctuation frequency of the mHC flow field and exemplary average velocity profiles as obtained by ultrasonic velocity profiling (UVP) can be found elsewhere.[17]

Having characterized the flow within the mHC experiments, the mHC experiments were conducted with APPs introduced into 100 L of ASW and systematically up-concentrated with the mHC. Separating the particle loaded foam at 3 different heights in the process (see Fig. 9: A, B, and C), the separation efficiency for the particles inserted at an initial concentration of 3.35 mg L^{-1} for different particle materials (MRP or MP-PMMA) is plotted in Fig. 10. When operating the mHC without bubbly flow, the concentration of separated particles was low and did not

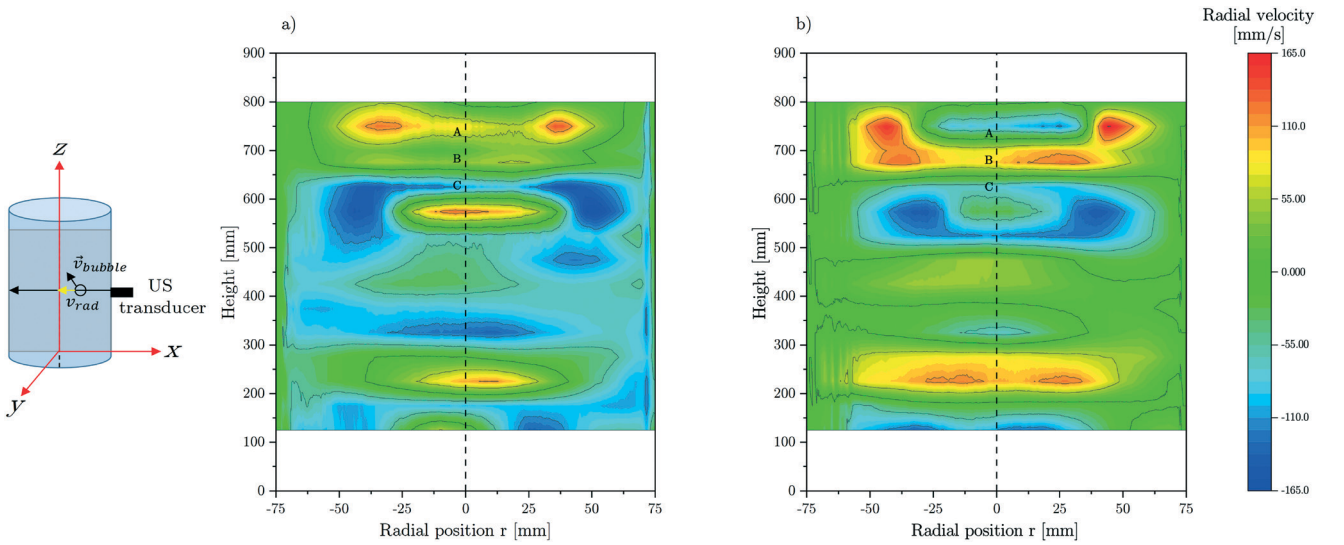

Fig. 9 Average radial velocity measured with UVP over the height of the hydrocyclone for a) the centerline and b) 1 cm offset. Letters A, B and C indicate APP extraction positions.

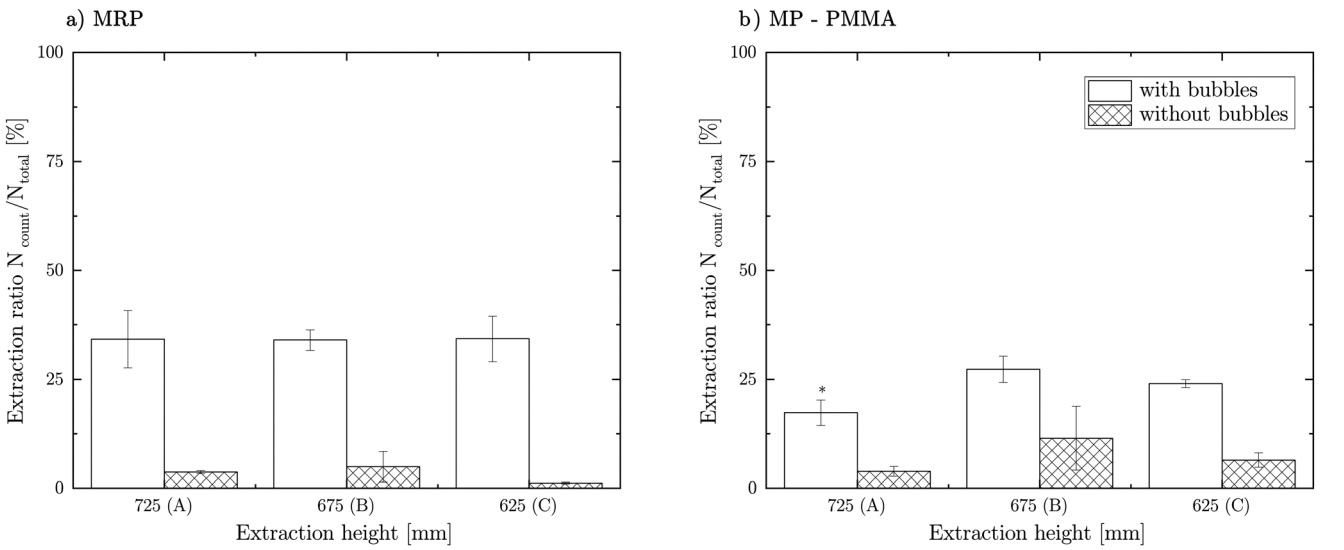

Fig. 10 Extraction ratio N_{count}/N_{total} as a function of extraction height of ASW with a particle concentration of 3.35 mg L^{-1} for a) MRP and b) MPs with and without bubbles.

significantly increase at the different extraction positions A to C. In the case of sampling at an expected favorable flow field section with the resulting velocity vector pointing towards the extraction point, an increase in particle concentration would be expected. At extraction point C, the average velocity vector points away from the extraction point which might lead to an opposing effect. Overall, the extraction ratio increased drastically ($p < 0.05$, $n = 3$) when the bubbly flow was applied for both types of APPs. This suggests that the radial velocity does not decrease the collection efficiency. More specifically, detachment events due to the hydrodynamics are less likely to be found. When the process was investigated over time, the extraction ratio did not decrease. The extraction of both APPs showed to be constant and stable over a period of 60 min (see Fig. 11). These are promising results in terms of stability and repeatability of the extraction technology.

Conclusion

Anthropogenic polymer particulates (APPs), namely MRP and MPs in the form of PMMA, showed to have a significant impact on the foamability of different watery media. As was reported by other researchers, MRP showed a floating top fraction forming spontaneously particle–foam cluster structures with an immobilized gas fraction. Once the particles protrude at the air–water bubble interface, the energy required for desorption becomes $\gg k_B T$. Moreover, in static foaming trials, an increased interaction and stabilization of the floating foam were found for

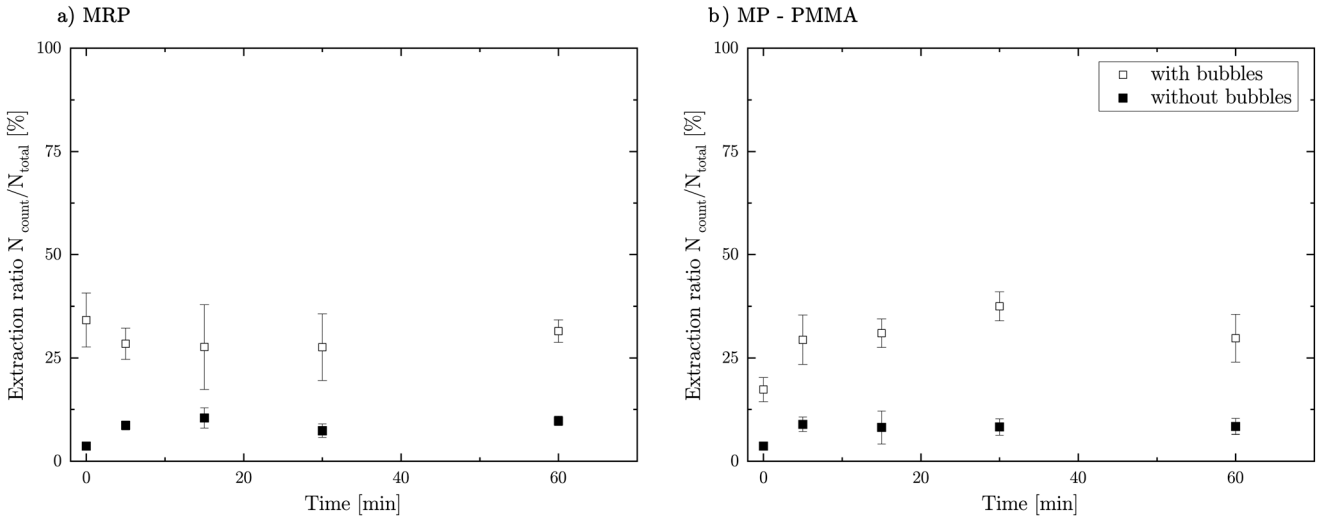

Fig. 11 Extraction ratio N_{count}/N_{total} of ASW with a particle concentration of 3.35 mg L^{-1} as a function of process time for a) MRP and b) MPs with and without bubbles. Extracted at point A.

MRP and PMMA in ASW and MilliQ water. In contrast, a significant decrease in the relative foam height was found for tap water. Thus, separation of these APPs from ASW was increased by applying a new technology of superimposed swirl flow and flotation in a modified hydrocyclone. A regular hydrocyclone would provide a density difference driven phase separation. The additional introduction of a bubbly co-flow promoted the APP–bubble interface interaction with subsequent flotation and particle loaded bubble concentration in the center of the upper hydrocyclone section. Thus as expected, the resulting particle extraction ratio was found to be significantly higher compared to that without bubbly flow. This newly designed separation processing principle demonstrates how microplastics with hydrophobic tendencies and low density differences to the medium can be separated or up-concentrated in an efficient way without the use of filters. The use of filters would be quite inefficient in the case of separation treatment of very low concentrated particle suspensions. Further, this technique shows high potential to serve as a pre-treatment step before subsequent filtration of wastewater containing microplastics.

Conflicts of interest

There are no conflicts to declare.

Acknowledgements

The authors thank Daniel Kiechl for his work on the conceptualization of the modified hydrocyclone. Further, J. V. thanks Prof. Lucio Isa for useful discussion on the visualization of the particles at the fluid interface. J. V. acknowledges funding from the European Union's Horizon 2020 research and innovation programme under the Marie Skłodowska Curie grant agreement 888076.

References

1 L. L. Halle, A. Palmqvist, K. Kampmann and F. R. Khan, Ecotoxicology of micronized tire rubber: Past, present and future considerations, *Sci. Total Environ.*, 2020, **706**, 135694.
2 Y. Cai, T. Yang, D. M. Mitrano, M. Heuberger, R. Hufenus and B. Nowack, Systematic Study of Microplastic Fiber Release from 12 Different Polyester Textiles during Washing, *Environ. Sci. Technol.*, 2020, **54**, 4847–4855.
3 J. Talvitie, A. Mikola, A. Koistinen and O. Setälä, Solutions to microplastic pollution – Removal of microplastics from wastewater effluent with advanced wastewater treatment technologies, *Water Res.*, 2017, **123**, 401–407.
4 I. A. Kane, M. A. Clare, E. Miramontes, R. Wogelius, J. J. Rothwell, P. Garreau and F. Pohl, Seafloor microplastic hotspots controlled by deep-sea circulation, *Science*, 2020, **368**, 1140–1145.
5 K. Enders, R. Lenz, C. A. Stedmon and T. G. Nielsen, Abundance, size and polymer composition of marine microplastics 10μm in the Atlantic Ocean and their modelled vertical distribution, *Mar. Pollut. Bull.*, 2015, **100**, 70–81.
6 Y. Chen, Y. Ling, X. Li, J. Hu, C. Cao and D. He, Size-dependent cellular internalization and effects of polystyrene microplastics in microalgae P. helgolandica var. tsingtaoensis and S. quadricauda, *J. Hazard. Mater.*, 2020, **399**, 123092.
7 Z. Zhang and Y. Chen, Effects of microplastics on wastewater and sewage sludge treatment and their removal: A review, *Chem. Eng. J.*, 2020, **382**, 122955.
8 S. Wagner, T. Hüffer, P. Klöckner, M. Wehrhahn, T. Hofmann and T. Reemtsma, Tire wear particles in the aquatic environment - A review on generation, analysis, occurrence, fate and effects, *Water Res.*, 2018, **139**, 83–100.
9 A. Wik and G. Dave, Occurrence and effects of tire wear particles in the environment - A critical review and an initial risk assessment, *Environ. Pollut.*, 2009, **157**(1), 1–11.

10 B. Quinn, F. Murphy and C. Ewins, Validation of density separation for the rapid recovery of microplastics from sediment, *Anal. Methods*, 2017, **9**, 1491–1498.
11 F. S. Degaffe and A. Turner, Leaching of zinc from tire wear particles under simulated sestuarine conditions, *Chemosphere*, 2011, **85**, 738–743.
12 J. C. Cullivan, R. A. Williams and C. R. Cross, Understanding the hydrocyclone separator through computational fluid dynamics, *Chem. Eng. Res. Des.*, 2003, **81**, 455–466.
13 L. Van Cauwenberghe, L. Devriese, F. Galgani, J. Robbens and C. R. Janssen, Microplastics in sediments: A review of techniques, occurrence and effects, *Mar. Environ. Res.*, 2015, **111**, 5–17.
14 M. Claessens, L. Van Cauwenberghe, M. B. Vandegehuchte and C. R. Janssen, New techniques for the detection of microplastics in sediments and field collected organisms, *Mar. Pollut. Bull.*, 2013, **70**, 227–233.
15 V. N. Paunov, Novel Method for Determining the Three-Phase Contact Angle of Colloid Particles Adsorbed at AirWater and OilWater Interfaces, *Langmuir*, 2003, **19**, 7970–7976.
16 D. R. Kester, I. W. Duedall, D. N. Connors and R. M. Pytkowicz, Preparation of artificial seawater, *Limnol. Oceanogr.*, 1967, **12**, 176–179.
17 L. Grob, E. Ott, L. Zeneli, Y. Takeda and E. J. Windhab *Investigation and comparison of fluid dynamics in a hydrocyclone using ultrasonic doppler velocity profiler*, unpublished, 2021.
18 C. Halsband, L. Sørensen, A. M. Booth and D. Herzke, Car Tire Crumb Rubber: Does Leaching Produce a Toxic Chemical Cocktail in Coastal Marine Systems?, *Front. Environ. Sci.*, 2020, **8**, 125.
19 F. Lu, Y. Su, Y. Ji and R. Ji, Release of Zinc and Polycyclic Aromatic Hydrocarbons From Tire Crumb Rubber and Toxicity of Leachate to Daphnia magna: Effects of Tire Source and Photoaging, *Bull. Environ. Contam. Toxicol.*, 2021, **107**(4), 651–656.
20 D. Boglaienko and B. Tansel, Wicking of light hydrophobic liquid phase from water by pulverized rubber: Theoretical and experimental analyses, *J. Hazard. Mater.*, 2017, **325**, 189–197.
21 N. Segre and I. Joekes, Use of tire rubber particles as addition to cement paste, *Cem. Concr. Res.*, 2000, **30**, 1421–1425.
22 M. Zanini and L. Isa, Particle contact angles at fluid interfaces: pushing the boundary beyond hard uniform spherical colloids, *J. Phys.: Condens. Matter*, 2016, **28**, 313002.
23 Y. Xing, M. Xu, X. Gui, Y. Cao, B. Babel, M. Rudolph, S. Weber, M. Kappl and H. J. Butt, The application of atomic force microscopy in mineral flotation, *Adv. Colloid Interface Sci.*, 2018, **256**, 373–392.
24 B. Wang and Y. Peng, The effect of saline water on mineral flotation - A critical review, *Miner. Eng.*, 2014, **66–68**, 13–24.
25 T. D. Blake and J. A. Kitchener, Stability of aqueous films on hydrophobic methylated silica, *J. Chem. Soc., Faraday Trans. 1*, 1972, **68**, 1435–1442.
26 Z. Dai, D. Fornasiero and J. Ralston, Particle-bubble collision models - a review, *Adv. Colloid Interface Sci.*, 2000, **85**, 231–256.
27 B. V. Derjaguin and S. S. Dukhin, Theory of flotation of small and medium-size particles, *Prog. Surf. Sci.*, 1993, **43**, 241–266.
28 K. L. Sutherland, Physical Chemistry of Flotation. XI. Kinetics of the Flotation Process, *J. Phys. Colloid Chem.*, 1948, **52**, 394–425.
29 G. Wang, G. M. Evans and G. J. Jameson, Bubble-particle detachment in a turbulent vortex I: Experimental, *Miner. Eng.*, 2016, **92**, 196–207.
30 R. Nauber, L. Büttner, K. Eckert, J. Fröhlich, J. Czarske and S. Heitkam, Ultrasonic measurements of the bulk flow field in foams, *Phys. Rev. E*, 2018, **97**, 013113.

